

**Title: Integration of Well Log, 3D Static Modeling, and Seismic Data in Characterization
of KUKO Field Offshore Niger Delta, Nigeria.**

This paper is a non-peer-reviewed preprint submitted to EarthArXiv

Authors:

- 1. Richard Alakuko, FUTAkure, Alakukorichard@gmail.com**
- 2. Moses Falowo, FUTAkure, moseso.falowo@gmail.com**

Abstract

The KUKO offshore field in Niger Delta exhibits complex structural deformation and faulting, impacting the exploration and development of reservoirs due to uncertain properties. This study employs an integrated approach combining 3D seismic, well logs, and reservoir modeling to characterize the field. The study is centered on establishing a template for future research, evaluating petrophysical properties, investigating structural styles, and constructing a 3D static reservoir model. Three hydrocarbon-bearing sand units (KUKO A, KUKO B, and KUKO C) were correlated across five wells using composite well log suites. Eight faults, including significant crestal faults (F2, F5, F7, and F8), were identified and interpreted from seismic data. Petrophysical results indicate favorable reservoir qualities with average effective porosity of 25% (KUKO A), 27% (KUKO B), and 24% (KUKO C), and average Net to Gross (NTG) values of 86% (KUKO A), 83% (KUKO B), and 80% (KUKO C). Hydrocarbon saturation averages 61% (KUKO A), 52% (KUKO B), and 58% (KUKO C). Estimated STOIP and recoverable oil volumes are as follows: KUKO A (STOIP: 642 MMbbl, Recoverable oil: 1901.9 MMBL), KUKO B (STOIP: 590 MMbbl, Recoverable oil: 1418.5 MMBL), and KUKO C (STOIP: 549 MMbbl, Recoverable oil: 349.1 MMBL). Amplitude maps superimposed on the depth-structure maps validated hydrocarbon potential, highlighting a prospect T. This study demonstrated the feasibility of integrating 3D seismic, well log data, seismic attributes, and 3D seismic, well log data, seismic attributes and 3D static reservoir modeling for accurate characterization of hydrocarbon reservoirs.

Keywords: Petrophysics, reservoir characterization, crestal faults, amplitudes, seismic attribute, Niger Delta

Introduction

The world will continue to need hydrocarbons for decades to come, even as we transition to a lower-carbon future. Oil and gas are not just fuels, they are feedstock for the chemical industry. (Alakuko, 2023). Recently, exploration and exploitation of unconventional reservoirs is on the increase and crucial in the portfolio of oil and gas industries in Niger Delta, these reservoirs are expected to secure the energy demand in the next decades. (Osaki, 2018). The principal goal of reservoir characterization is to outsmart nature and enhance hydrocarbon recovery with fewer optimally placed wells at minimum cost (Halderson and Damsleth, 1993). Reservoir characterization is continually evolving with time, basically it has tremendously evolved in three generations based originally in petrophysics, then on geologic analogs, and more recently on multidisciplinary integration (Alao et al., 2013). Recently, reservoir characterization approach made extensive use of 3D seismic amplitude anomalies, Reservoir properties modeling and Sequence stratigraphy in defining fields. This multidisciplinary approach was employed in this research work.

The study adopts a multi-disciplinary approach of data integration using 3D seismic data, well logs, deviation and checkshot data with 3D static models to effectively characterize the hydrocarbon reservoirs of the field in order to predict the reservoir parameters, subsurface structural geometry, stratigraphy and hydrocarbon trapping potential of the Field.

Location of Study Area

The study area “KUKO” field is located in the shallow offshore depobelt of the Niger Delta (Fig. 1). The field lies within the transitional zone of the Niger Delta which is characterized by a mix of normal and compressional faults.

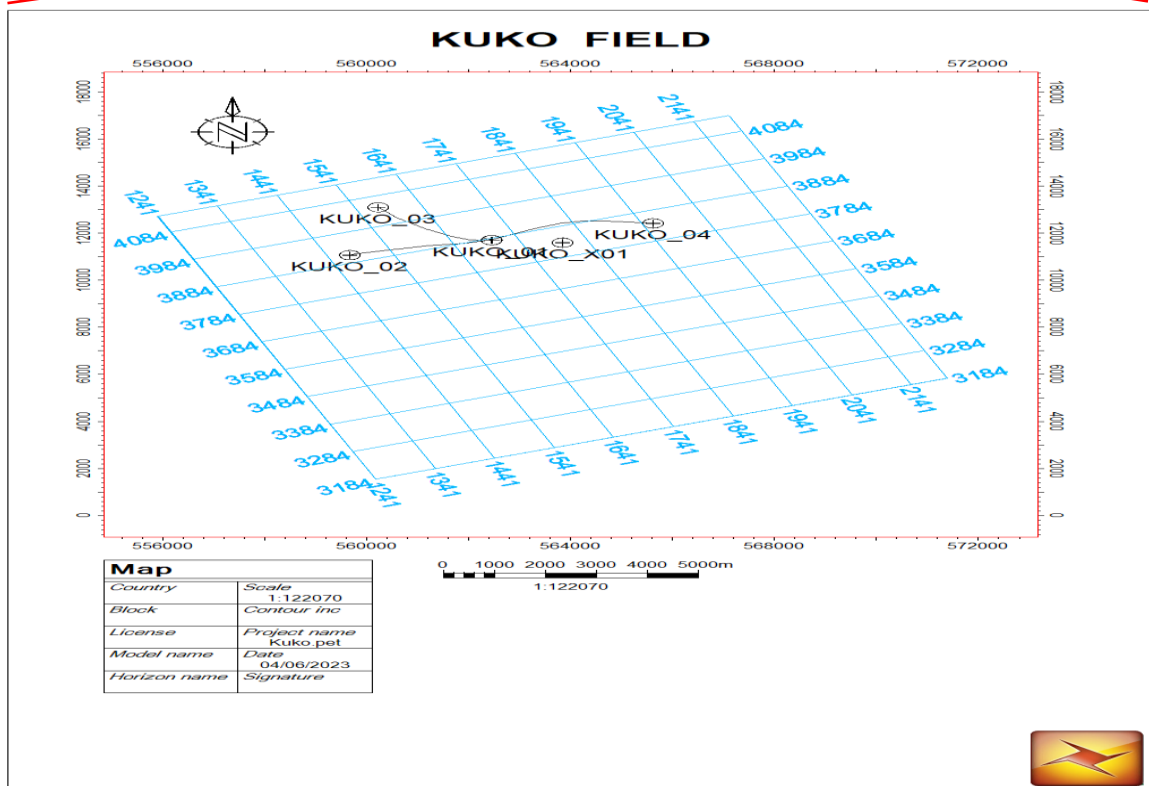
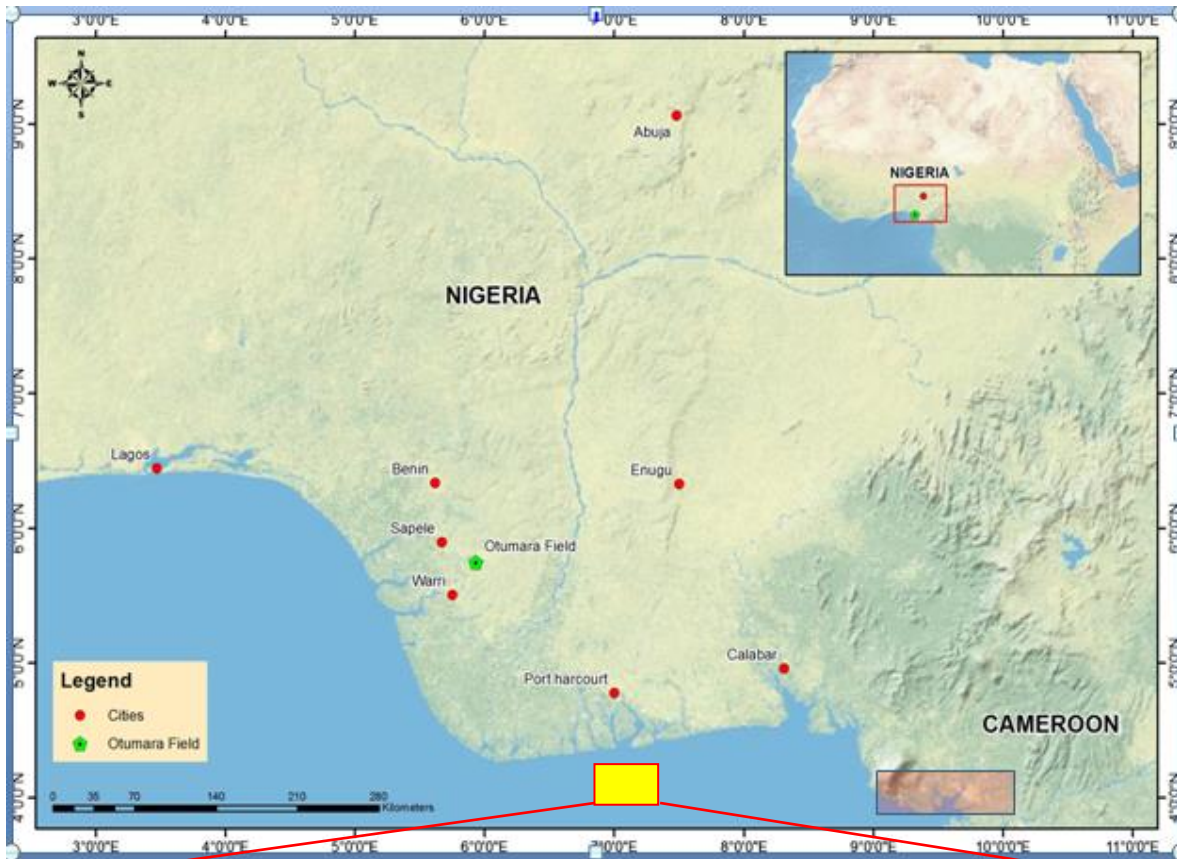


Figure 1: Approximate location and Base map of KUKO field in the Niger delta, Nigeria.

Objective of Study

The objectives of the study include, but are not limited to:

1. Evaluate reservoir properties such as porosity, permeability, and the geometry of the reservoir including faults and facies distribution which are the primary characteristics responsible for the migration of hydrocarbon;
2. Generate seismic attribute maps such as RMS, Maximum Amplitude, and Average Energy to identify sweet spots in the study area in order to delineate prospects;
3. Define a 3D static model for the hydrocarbon-bearing reservoirs; and
4. Make recommendations for future exploration & production activities in the study area.

Geologic settings of the Niger Delta

The Niger Delta basin is one of the largest sub-aerial basins in Africa. It is an extensional rift basin located in the Gulf of Guinea on the passive continental margin near the western coast of Nigeria with suspected or proven access to Cameroon, Equatorial, Guinea, and São Tomé and Príncipe. The delta evolution is characterized by southwest progradation forming depobelts which depict the most active portion of the delta at each stage of its development from the Eocene to the present (Doust and Omatsola, 1990).

Three major depositional cycles have been identified within Tertiary Niger Delta deposits (Short and Stauble, 1967; Doust and Omatsola, 1990). The first two, involving mainly marine deposition, began with a middle Cretaceous marine incursion and ended in a major Paleocene marine transgression. The second of these two cycles, starting in late Paleocene to Eocene time, reflects the propagation of a “true” delta, with an acute, wave and tide-dominated coastline.

The Niger Delta basin is characterized by tripartite stratigraphy representing prograding depositional facies that are distinguished mostly on the basis of sand-shale ratios (Fig. 2). The three subsurface lithostratigraphic units are:

- i. The Akata Formation

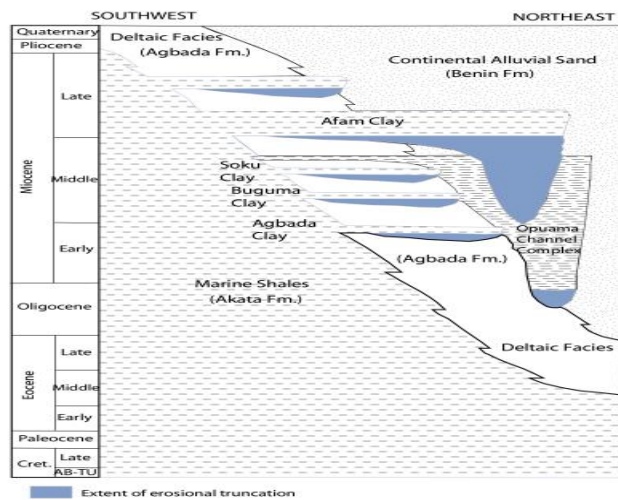


Figure 2: Stratigraphic column showing the three formations of the Niger Delta. (Doust and Omatsola, 1990).

The Akata Formation is characterized by dark gray shale and silts with rare streaks of sand of probable turbidite flow origin; it is estimated to be 6,400 m thick in the central part of this clastic wedge (Doust and Omatsola, 1989). The shale is undercompacted and may contain lenses of abnormally high-pressure siltstone or fine grained sandstone, the Akata Formation is believed to be the main source rocks of the eastern part of the Delta.

ii. The Agbada Formation; and

This unit constitutes the middle part of the tripartite Niger Delta stratigraphic succession and represents the actual deltaic portion of the sequence. It is made up of paralic siliciclastics that is over 3700m in thickness (Magoon and Dow, 1994). The Agbada formation overlies the Akata and it is the major petroleum bearing unit. The formation is strongly diachronous, ranging in age from Eocene (lower-middle tertiary) to recent. The mangrove swamp to coastal barriers and fluviomarine zones of the present-day delta constitute the surface exposure of recent age.

iii. The Benin Formations

This unit consists predominantly of continental fluvial sands that underlie an extensive area of southern Nigeria typified by the sands around Benin City where it is estimated to be 3050m thick. The Benin Formation is reconstructed as the upper and lower flood (delta) plain setting which also includes deltaic, estuarine, lagoonal, and fluviolacustrine sub-environments.

Methodology

This gives a detailed procedure and data set utilized in this study, these data set include;

1. A 3D Seismic data (SEG Y Format), 2. Well Header, 3. Well Deviation Data (ASCII format), 4. Composite geophysical well logs for five (5) wells, 5. Well Tops and 6. Checkshot Data.

The methodology of this study involves data gathering and analysis of the data using Petrel™ software by Schlumberger. Quality check was carried out to ascertain that there are no discrepancies in the data employed.

The workflow utilized in this study is depicted below in a diagrammatic format (Fig. 3).

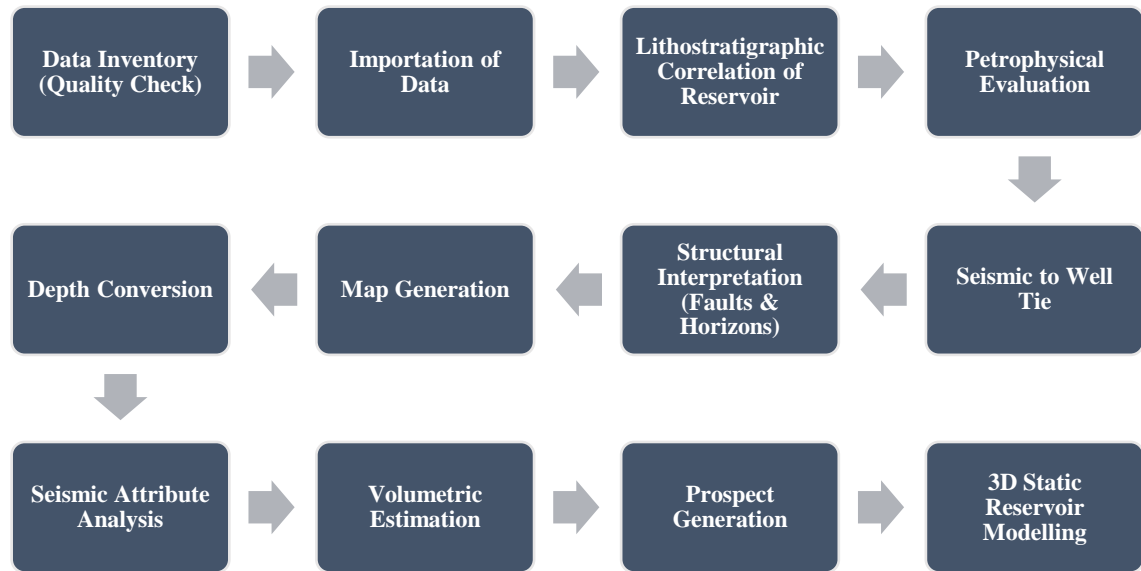


Fig. 3: Detailed workflow utilized in the characterization of KUKO field (Modified after Yuan *et al.*, 2011).

Importation of data

After quality check of well data, a well folder was created, then the well header which allows the display of well positions on the base map was loaded first on petrel creating a path for other well data (logs, deviation, checkshot etc.), the log data which was in the ASCII data format was also imported into PETREL software using the appropriate format. The seismic data in SEG Y format was also imported into PETREL.

Lithostratigraphic correlation of reservoir

The gamma ray log was used for lithological discrimination. The first stage for this correlation was a visual correlation of the well logs, which was accomplished by preparing a correlation panel. Reservoirs were delineated, and the gamma ray signature was used to correlate the reservoirs across the 5 KUKO field wells. However, the gamma ray log was not used alone; it was combined with the resistivity and porosity logs to improve interpretation accuracy. The fluid type in the reservoir was determined using the resistivity log because high resistivity zones indicate the presence of hydrocarbons or freshwater, and because the reservoirs of the Agbada formation are of

marine origin and thus should contain saline water, high resistivity zones were delineated as hydrocarbon bearing and low resistivity zones as saline water bearing, using knowledge of the geology of the study area.

Petrophysical evaluation

In order to have better understanding and characterize the KUKO field reservoirs, the tool of petrophysics was employed to evaluate the reservoir properties, the well logs provided information on the reservoir's in-situ attributes, and mathematical models and equations were employed in order to determine the reservoir's quantitative properties. This study evaluated petrophysical parameters such as shale volume, Net to Gross, porosity, permeability, hydrocarbon saturation, and water saturation.

Well to seismic tie

Seismic well ties are completely crucial part of interpretation and modelling. Well logs samples and seismic data are of different units. Well logs are in unit of depth (ft. or m) while the seismic data are sampled in the unit of time (ms), it's therefore imperative to find a relationship between these data of different unit so that what is visualized on the well logs is populated on the seismic. We do a well tie in which we produce a synthetic that is compared with the original seismic, in order to accurately tie well top markers to a specific event on the seismic profile. The seismic well tie tool was used from the process pane, a sonic calibration was created combining the check shot of KUKO 01 log which is the control well and its sonic log. In this study the Ricker wavelet was utilized to extract a wavelet.

Fault and Horizon mapping

Faults are structural characteristics of crustal rocks effectuated by tectonic stress while horizons are well-known seismic events that are mapped across the seismic volume, they refer to isochronous time surfaces corresponding to events deposited at the same time. Fault can both act as a barrier to the flow of hydrocarbons and serve as pathways for their migration, giving them a dual purpose. Horizons could be the top and or the base of a reservoir, a fluid contact or a geologic event which coincides with a particular reflector (peak, trough or two-way crossing) on the seismic volume. Faults are identified on seismic based on the subsequent criteria; reflection discontinuity at fault plane, vertical displacement of reflection, abrupt termination of seismic events/ truncations, breaks in reflection events, abrupt lateral velocity changes, overlapping of reflection events and pattern change of reflection events across a fault.

Fault interpretation in this study was done by drawing of fault segments, on areas where fault identification criteria were seen on the seismic volume. The fault interpretation was carried out in the seismic interpretation window which gives a 2D view of the seismic data. At 20 in-line interval, faults were picked first on the inlines before being

traced across the crosslines, tracking was used to serve as a guide to pick faults on subsequent inlines and crosslines and they were named.

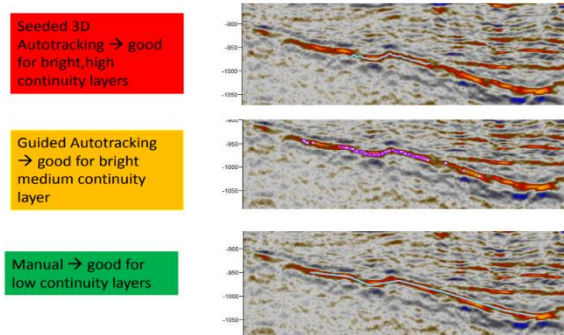


Figure 4: Seismic section showing how horizons are mapped (Rahmadi, 2010).

Seismic attribute generation

Seismic attributes are important because they enable interpreters to enhance information that might be more subtle in a traditional seismic image, leading to a better geological or geophysical interpretation of the data. Volume and surface attributes are the two types of seismic attributes that are available. The available attributes in each process are organized by several libraries, which attempt to group attributes with similar outputs.

Libraries in the attributes pane include basic attributes, complex attributes, stratigraphic methods, signal processing, structural methods, amplitude attribute, depth conversion, AVO attributes, crossplot, and pre-secondary AVO attributes. The mean amplitude attribute, leads to the delineation of bright spots, flat spots, polarity reversals, and dim spots, which show the presence of hydrocarbons. The places that were delineated are called direct hydrocarbon indicators (DHIs). The Variance attribute was also utilized in the extraction of an edge volume from an input seismic volume. This attribute is a coherency attribute that enables the identification of faults. RMS amplitude attribute which computes RMS on instantaneous trace samples over a specified window was used to generate amplitude maps.

Static reservoir modeling

Static models demonstrate how structural features appears in the subsurface. Static models are also spatial representation of facie, porosity, permeability and saturation that incorporates all key heterogeneities and reservoir connectivity that can influence reservoir performance. In generating the static reservoir model for this project, all the available dataset were integrated. Static models can be grouped mainly into structural model, stratigraphic model and lithological/property model.

Structural modelling

Fault modelling

This forms the first stage of critical decision making where interpreted faults were quality checked to determine if they were geologically and geometrically reasonable to impact flow behaviour. Due to the absence of fault transmissibility data all faults were assumed to be sealing.

Pillar gridding and boundary definition

To define the horizontal resolution and the skeleton framework of the model a pillar grid with increments of 100 m was used as well as setting the major bounding faults as part of the grid boundary. The trends were set to the major North-South trending faults and its perpendicular faults respectively.

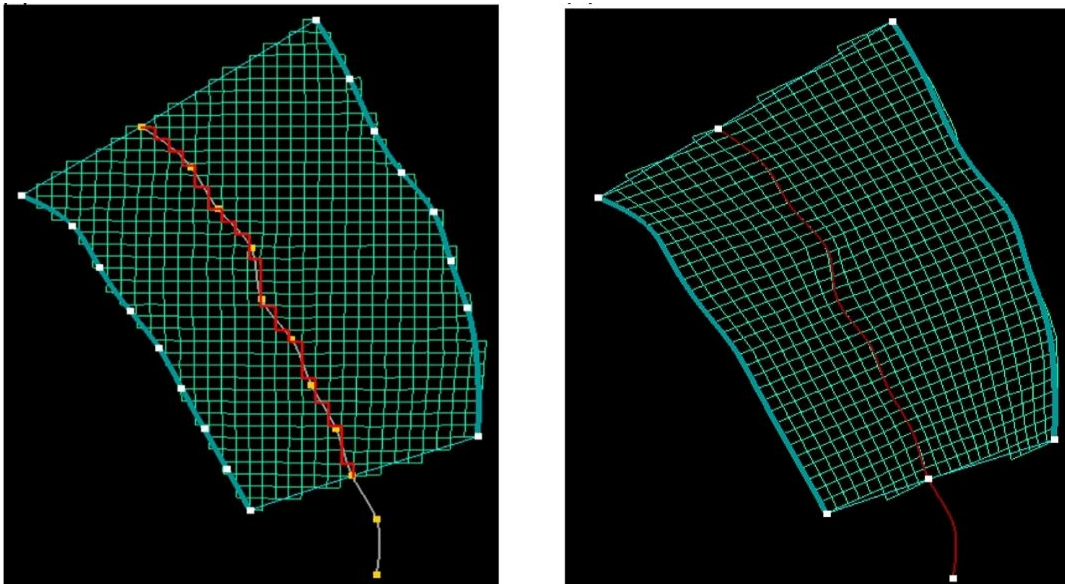


Figure 5: Pillar gridding between faults for modelling.

Horizon modelling and depth conversion

Based on well and seismic interpretation, horizons were created in their correct stratigraphic sequence. Well tops were used to define horizon tops with the horizon surfaces as inputs. Based on literature, the basal contact types were set accordingly incorporating relevant faults pertaining to the horizons. A Domain conversion of the 3D grid and fault model was done using a velocity model to bridge the gap between time and depth using the seismic reference datum to create a realisation of the subsurface independent of time. The layer cake method for depth conversion was used for this process with the velocity model $V=V_0+KZ$ used due to the relative relationship between depth and time, velocity values for K becomes negative. The resulting 3D grid was used throughout the project.

Facies modelling

Facies models are encapsulated summaries of sedimentation in a depositional environment. The models are therefore finds usefulness in the estimation of sediments and understanding of the sedimentary environment. Gamma ray log were up scaled, then the up scaled gamma ray log is used to compute the facies model. To define the boundary between shale and sand, the shale baseline was set at 75gAPI. Shale corresponds to values greater than 75, while sand corresponds to values less than 75. Well logs can be used in deterministic and stochastic modelling after being up-scaled. Due to the sparse well data, sequential indicator stimulation was used for this project, which is a stochastic technique.

Petrophysical modelling

Petrophysical models rely solely on well data for reservoir characterization. The primary data sets for building the petrophysical model are well logs. It depicts the distribution of porosity, permeability, and water saturation throughout the reservoir. The Gaussian random function stimulation was used to generate a model for each of the properties using the up scaled well logs computed from the petrophysical evaluation. The Gaussian random function stimulation method used in this study is a krig-based stochastic method. It necessitates a variogram and takes into account the distribution of the input data (up-scaled logs).

Volumetric estimation

The volume of hydrocarbon determines whether or not a reservoir is economically viable. Volumes can be calculated exactly within zones, segments and user defined boundaries. The average petrophysical properties of the reservoir obtained from the petrophysical analysis of the well logs were used to estimate the STOIP, GIIP and UR of the reservoirs of the KUKO field. The volume estimation was computed using the following equations:

$$\text{Net} = \text{Bulk volume} \times \text{NTG}$$

$$\text{Pore} = \text{Net volume} \times \text{Porosity}$$

$$\text{HCPVo} = \text{Pore volume} \times \text{So}$$

$$\text{HCPVg} = \text{Pore volume} \times \text{Sg}$$

$$\text{STOIP} = \text{HCPVo}/\text{Bo} + (\text{HCPVg}/\text{Bg}) * \text{Rv}$$

$$\text{GIIP} = \text{HCPVg}/\text{Bg} + (\text{HCPVo}/\text{Bo}) * \text{Rs}$$

$$\text{Recoverable oil} = \text{STOIP} * \text{RecFo}$$

$$\text{Recoverable gas} = \text{GIIP} * \text{RecFg}$$

Results and discussion

Three (3) hydrocarbon-bearing reservoirs, KUKO A, KUKO B, and KUKO C, were delineated (Fig. 6) using the convectional triple combo log. The hydrocarbon bearing reservoir was encountered in all the five wells of the field (KUKO_01, KUKO_02, KUKO_03, KUKO_04 and KUKO_X01). KUKO A lies approximately between the depth interval of 2272 m and 2657 m, KUKO B also lies approximately between the depth interval of 1930 m and 2289 m while KUKO C lies approximately between the depth interval of 1825 m and 2115 m (Fig. 7).

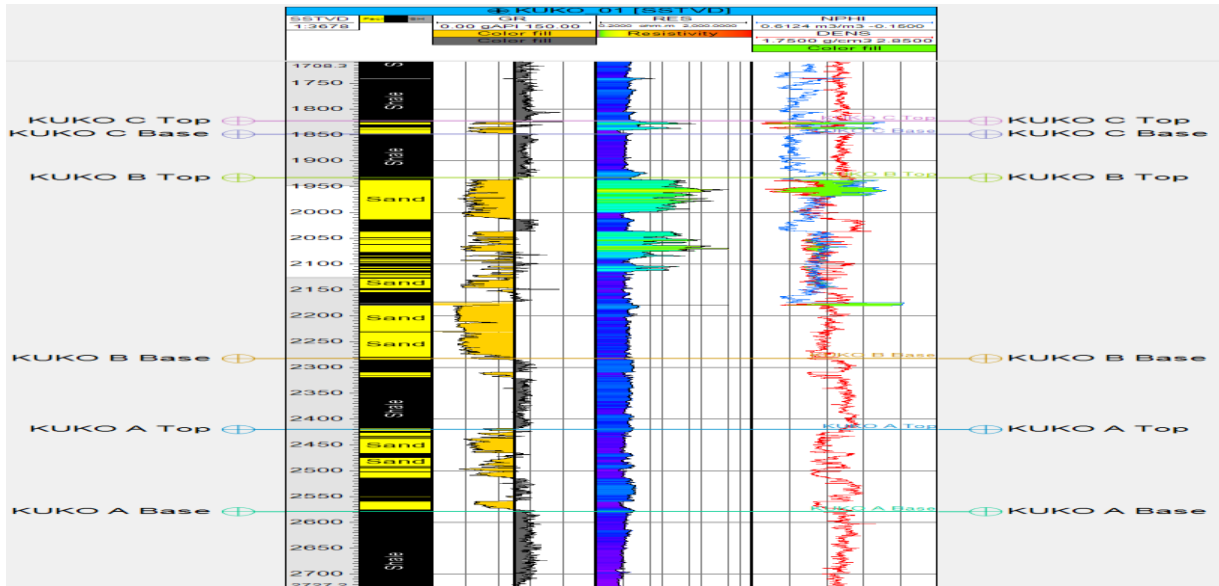


Figure 6: Well KUKO_01 with the three hydrocarbon bearing reservoir candidates mapped (KUKO A, KUKO B & KUKO C).

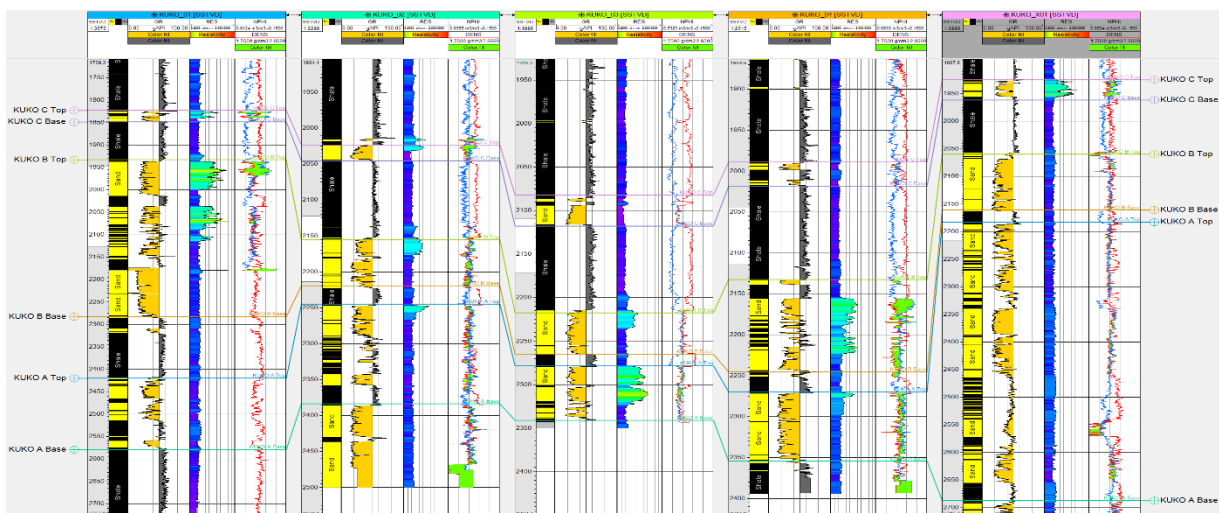


Figure 7: Well log correlation panel showing the continuity of KUKO A, KUKO B and KUKO C.

Petrophysical analysis

The petrophysical evaluation results indicate that the hydrocarbon reservoirs are of high quality. The average effective porosity measurements (Table 1-5) suggests that, the reservoirs possess a well-connected network of pores. Furthermore, the reservoirs show an average water saturation of 38.62% for KUKO A, 47.03% for KUKO B, and 41.45% for KUKO C, indicating that there is room for further hydrocarbon accumulation. Moreover, the average net-to-gross (NTG) values for KUKO A, KUKO B, and KUKO C are 86.59%, 83.41%, and 80.43%, respectively. The high NTG values signify that the reservoirs are very clean and possess a high sand-to-shale ratio, which translates to higher potential for hydrocarbon recovery. The petrophysical evaluation demonstrates that the hydrocarbon reservoirs under study are of good quality and possess favourable characteristics for hydrocarbon production.

Table 1: Summary of the petrophysical result for KUKO_01

Reservoir Sand	KUKO A	KUKO B	KUKO C
Top (m)	2465.07	1929.66	1825.37
Base (m)	2578.87	2286.29	1848.85
Gross Thickness (m)	113.8	356.63	23.48
Shale Volume (%)	17.94	25.67	22.31
Net to Gross (%)	82.06	74.33	77.69
Effective Porosity (%)	20.72	24.74	28.93
Water Saturation (%)	51.62	41	42.33
Permeability (mD)	1477.18	2681.47	4160.15
Hydrocarbon Saturation (%)	48.38	59	57.67
Fluid type	Oil + water	Oil + water	Oil + water

Table 2: Summary of the petrophysical result for KUKO_02

Reservoir Sand	KUKO A	KUKO B	KUKO C
Top (m)	2342.88	2154.83	2012.91
Base (m)	2357.07	2288.95	2044.13
Gross Thickness (m)	14.19	134.12	31.22
Shale Volume (%)	5.37	17.42	15.16
Net to Gross (%)	94.63	82.58	84.84
Effective Porosity (%)	31.2	21.2	24.9

Water Saturation (%)	35.09	60.71	40.79
Permeability (mD)	1512.1	1806.98	2050.97
Hydrocarbon Saturation (%)	64.91	39.29	59.21
Fluid type	Oil + water	Oil + water	Oil + water

Table 3: Summary of the petrophysical result for KUKO_03

Reservoir Sand	KUKO A	KUKO B	KUKO C
Top (m)	2279.33	2215.52	2085.77
Base (m)	2337.47	2287.28	2114.84
Gross Thickness (m)	58.14	71.76	29.07
Shale Volume (%)	18.29	12.68	20.46
Net to Gross (%)	81.71	87.32	79.54
Effective Porosity (%)	22.62	19.65	22.54
Water Saturation (%)	43.78	49.36	52.26
Permeability (mD)	2061.88	1435.91	1814.13
Hydrocarbon Saturation (%)	56.22	50.64	47.74
Fluid type	Oil + water	Oil + water	Oil + water

Table 4: Summary of the petrophysical result for KUKO_04

Reservoir Sand	KUKO A	KUKO B	KUKO C
Top (m)	2272.03	2131.79	1990.07
Base (m)	2354.27	2243.39	2017.98
Gross Thickness (m)	82.24	111.6	27.91
Shale Volume (%)	8.39	21.64	21.93
Net to Gross (%)	91.61	78.36	78.07
Effective Porosity (%)	19.12	35.14	21.97
Water Saturation (%)	27.86	54.43	44.18
Permeability (mD)	1871.71	511.46	1433.92

Hydrocarbon Saturation (%)	72.14	45.57	55.82
Fluid type	Oil + water	Oil + water	Oil + water

Table 5: Summary of the petrophysical result for KUKO_X01

Reservoir Sand	KUKO A	KUKO B	KUKO C
Top (m)	2342.37	2057.37	1926.19
Base (m)	2657.58	2167.73	1959.22
Gross Thickness (m)	315.21	110.36	33.03
Shale Volume (%)	17.06	5.55	18.01
Net to Gross (%)	82.94	94.45	81.99
Effective Porosity (%)	33.83	36.41	25.66
Water Saturation (%)	34.77	29.65	27.69
Permeability (mD)	4130.52	5178.56	2318.77
Hydrocarbon Saturation (%)	65.23	70.35	72.31
Fluid type	Oil + water	Oil + water	Oil + water

Seismic to well tie

The well-to-seismic tie, as well as the correlation within the field of study, yield a very good result despite the fact that the near-stack seismic data is nearly at zero offsets. A Ricker 20Hz wavelet was used for convolution, and a 10ms bulk shift was performed to ensure that the synthetic ties to the original seismogram (Fig. 8). The tops of sand units in KUKO field generated distinct troughs which were used for horizon correlation after a proper well-to-seismic tie. The seismic events that correspond to the three reservoirs of sand through the synthetic seismogram were then mapped across the field.

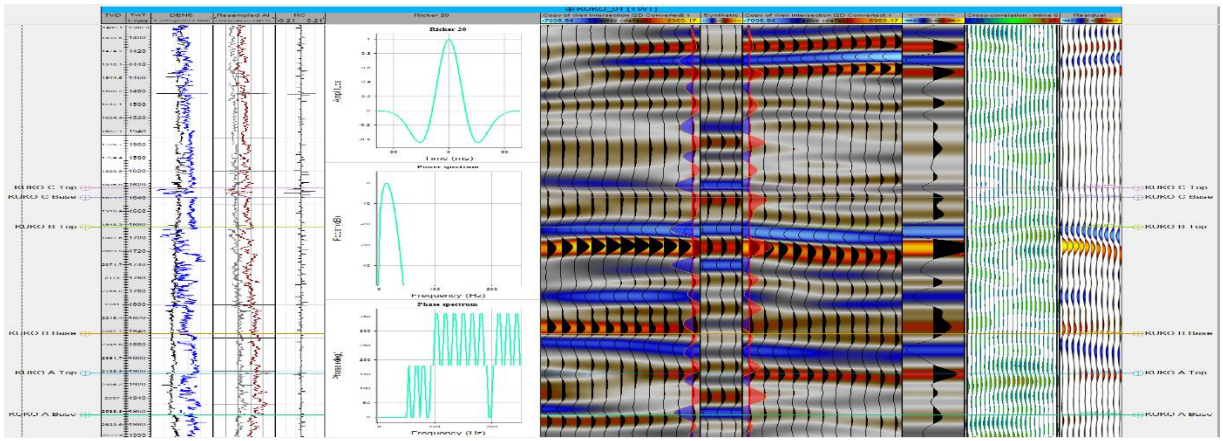


Figure 8: Synthetic seismogram generated to ensure an excellent matching of the well log and the seismic.

Fault and horizon mapping

Faults were mapped perpendicular to the fault dip direction based on the abrupt termination and dip of seismic events. A discontinuous cube (variance cube) time slice was used to properly image the faults. The variance edge seismic attribute correlates well with faults and fractures in the study area. A total of eight (8) faults labeled F1, F2, F3, F4, F5, F6, F7, and F8 were mapped across the seismic inline, most of which are crestal and major growth faults that trend east-west. F2, F7, and F6 were the major structure building faults, which correspond to the growth faults in the area. Antithetic and synthetic faults were observed. These faults act as hydrocarbon traps as well as secondary migration conduits. The mapped horizons are characterized by Low-to-high or variable amplitude reflections, with poor-to-low continuity (Fig. 9). In some places, it is disturbed by some truncations which are more of fault related.

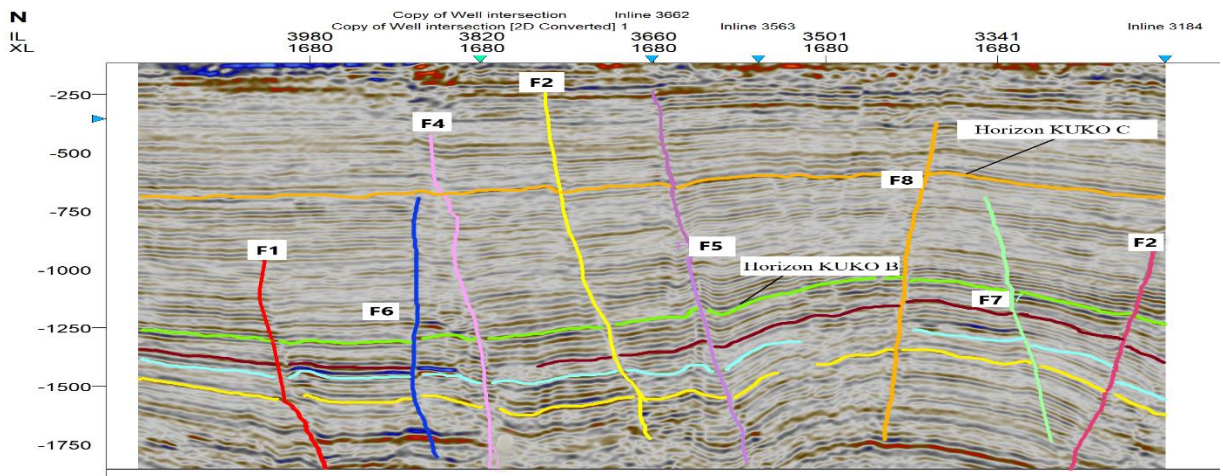


Figure 9: Seismic section showing the mapped horizons and faults. Note; disturbances marked by some truncations which are likely fault related than lithologic heterogeneity.

Seismic structural maps

Time structural and depth structural maps were created. The mapped horizons were converted to surface to produce a structural time map; the structural time maps was then converted to depth maps using the polynomial function generated from the checkshot plot (Fig. 10). The structural depth maps shows similar structural configurations to the time structural maps that were generated. The maps revealed the fault distribution with 7 of the 8 faults mapped being evident on the map with the prominent major fault trending in the NW (Northwest)-EW (Eastwest) direction.

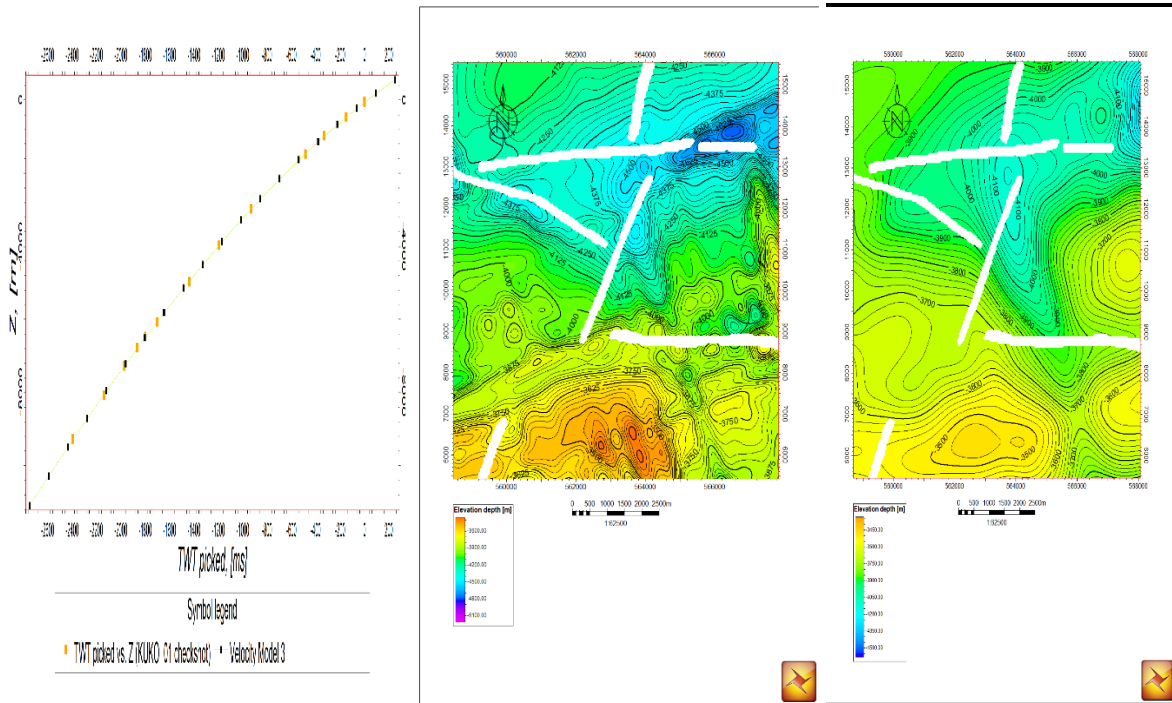


Figure 10: (a) Check shot (Z vs TWT) data generated for the field of study; (b) KUKO C time map; (c) KUKO C depth map.

Seismic attribute analysis

In order to improve the spatial prediction of structural and stratigraphic features as well as petrophysical and geomechanical properties throughout the reservoir, seismic attribute analysis was employed. Three attributes (amplitude, average energy, root mean square) were extracted and displayed as flattened maps (Fig. 11). Root mean square (RMS) amplitude, instantaneous frequency and interval average maps were extracted on seismic events with pronounced bright and dim spots. These maps were used to establish areas of high amplitude, which are indicative of hydrocarbon accumulation. These high amplitude pattern (bright spots) were mostly observed at the bottom portion of the map away from the well locations and were referred to as a 'lead'.

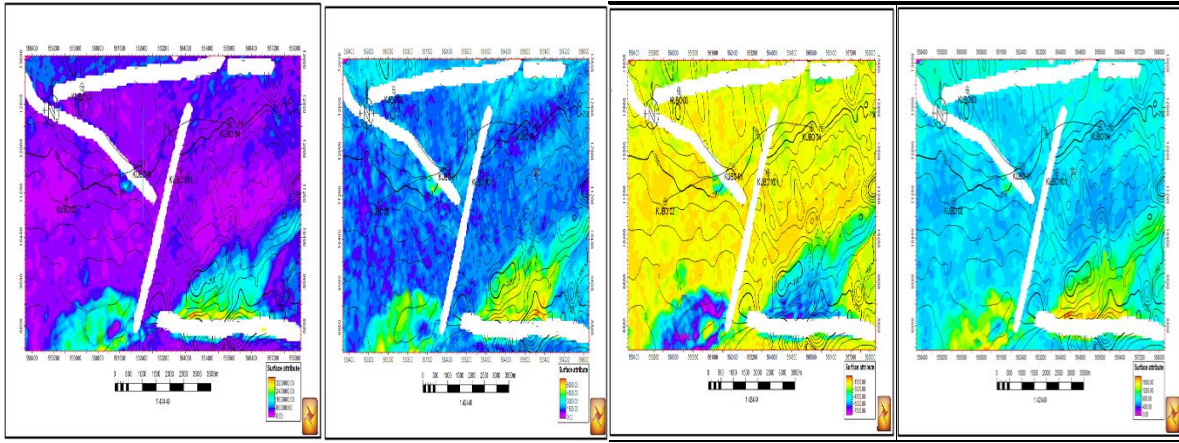


Figure 11: (a) Average energy, (b) Maximum amplitude, (c) Minimum amplitude & (d) RMS amplitude surface attribute map showing amplitude variation.

Static reservoir model

A structural framework built in depth domain was created as the first stage of structural modelling. Also developed were horizon modeling and fault framework modeling. The fault framework model includes the eight faults that impact the reservoirs, they are F1, F2, F3, F4, F5, F6, F7 and F8 while the horizon model includes all three structural maps in depth. Fig. 12 shows the pillar gridding of the faults and the top, mid and base skeletal framework of the model. The distribution algorithm used was sequential indicator simulator, the variogram type was exponential and the nugget was set to 0.1. The Anisotropy range were; 3000 in major direction, 1500 in minor direction, vertical 10 and Azimuth of 45. This was based on the results of data analysis from analog data within the Niger delta. Different petrophysical properties models were created (Fig. 13).

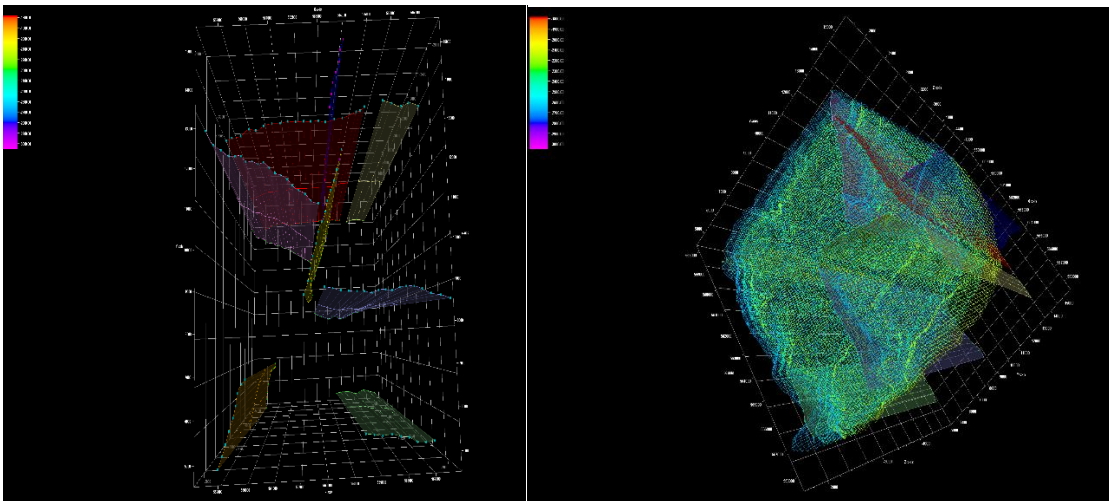


Figure 12: (a) Fault grid;(b) Pillar gridding showing the Top, Mid and Base skeletal framework.

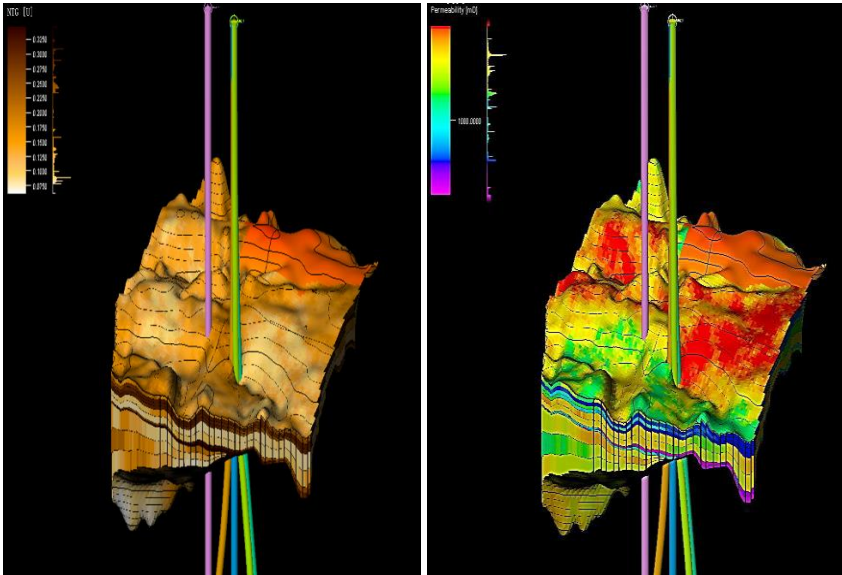


Figure 13: (a) 3D model of the net to gross; (b) 3D model of effective porosity distribution within delineated KUKO reservoirs.

Fluid contacts model

Water and oil were the fluids encountered in KUKO A, KUKO B and KUKO C. (Fig. 14) shows the Oil-Water contact (OWC) in the reservoirs. KUKO A is composed in almost equal proportion of water and oil while KUKO B is predominantly composed of oil but also contains water and KUKO C is almost entirely composed of oil with little water, the oil reserve occupies the green portion of the reservoir while the water reserve occupies the blue portion of the reservoir on fluid contact model.

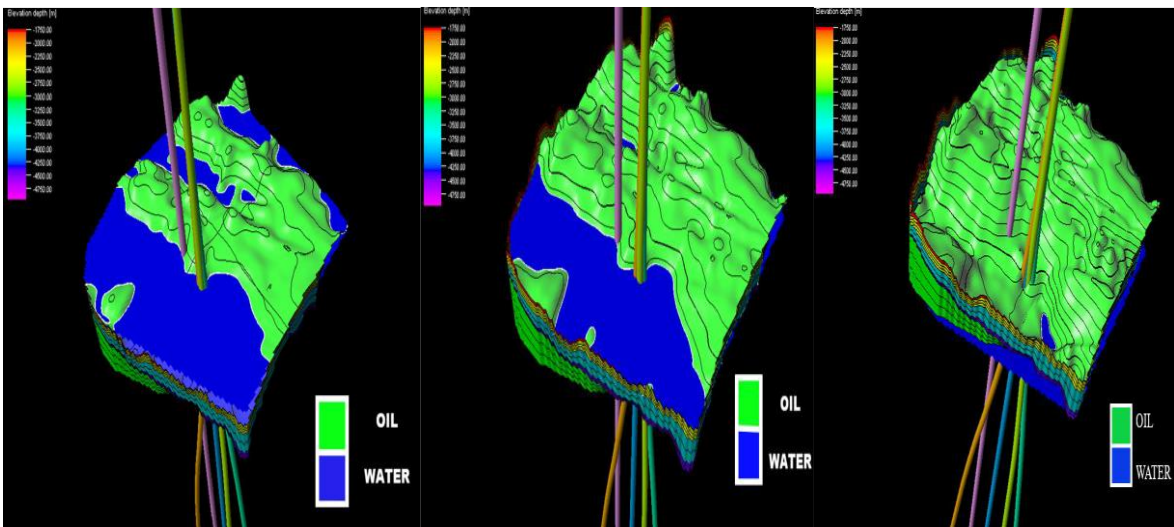


Figure 14: 3D model of the Oil Water Contact within delineated (a) KUKO A; (b) KUKO B and (c) KUKO C reservoir.

Prospect delineation

The prospect *TORERA* (T) (Fig. 15) delineated was established by integrating the attribute map generated, the depth structural maps as well as the 3D static model generated. The attribute adopted was the RMS surface attribute, and regions of anomalous attribute variation, typically characterized by a bright spot, coincided with areas that were structurally high on the depth structural map as well as regions that were highly saturated with hydrocarbon from fluid contact and hydrocarbon saturation on the static model created. The faults that bound the prospect T forms anticlinal structure which are great structural trap for the hydrocarbon in place. In order to access the identified prospect T, KUKO_X02 should be drilled as an exploratory well.

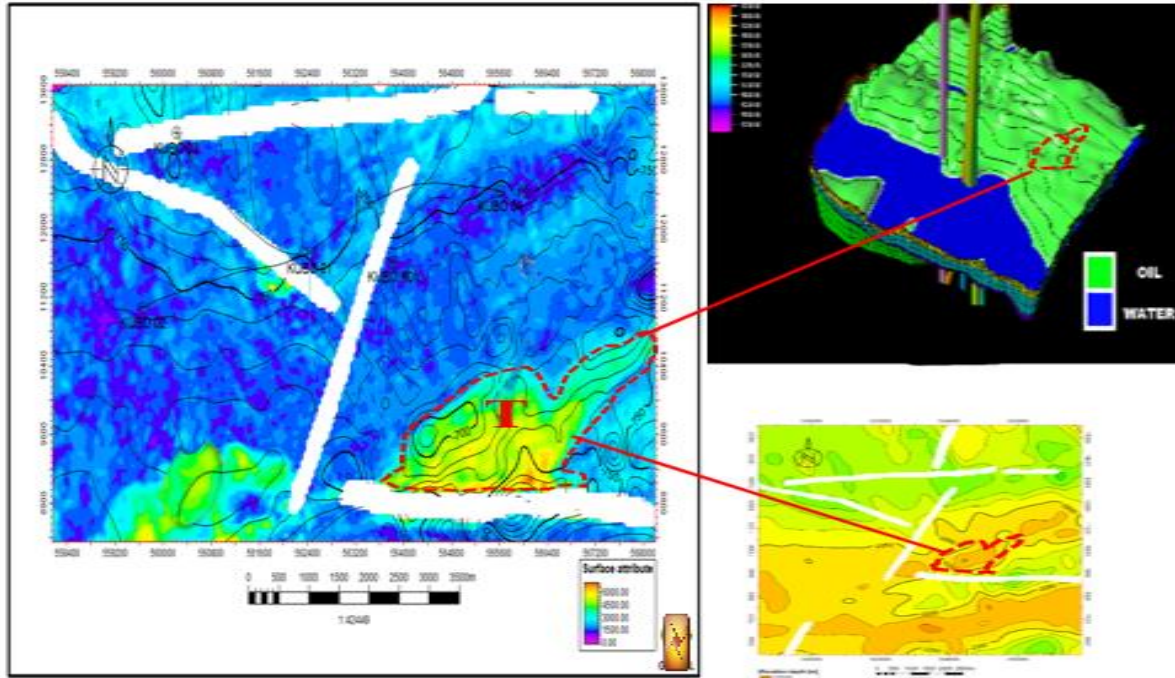


Figure 15: The three (3) approaches utilized in delineating prospect T

Volumetric estimation

The Stock tank oil initially in place (STOIP) estimation with the model based volumetric calculation for KUKO A, KUKO B, and KUKO C was 642.32 MMbbl, 590.34 MMbbl and 549.75 MMbbl respectively. The recoverable oil for KUKO A, KUKO B, and KUKO C were estimated to be 1901 MMBL, 1418 MMBL, and 349 MMBL. (Table 6) shows a summary of the volumetric estimation.

	KUBO A	KUBO B	KUBO C
STOIP [$*10^6$ sm³]	642.3244	590.3370	549.7543
Recoverable Oil [$*10^6$ sm³]	1901.945071	1418.508635	349.1103317
Pore Volume [$*10^6$ rm³]	5449.008227	4074.455714	993.2680609
Net Volume [$*10^6$ m³]	25009.48329	18627.7057	4412.688905
HCPV Oil [$*10^6$ rm³]	3138.209322	2340.539213	576.0320389
Bulk Volume [$*10^6$ m³]	25009.48329	18627.7057	4412.688905

Conclusion

This study shows the feasibility and versatility of integrating seismic data, well logs with a 3D static geological model in characterizing KUKO field. The structural interpretation of the seismic data revealed East West trend of major faults which corresponds to the general trend of growth faults in the Niger Delta. Fault-assisted anticlinal traps were identified in the field as the major structural trap.

From the well log data, 3 hydrocarbon-bearing reservoirs were delineated. Petrophysical and 3D static model generated, generally affirms the good petrophysical quality of the reservoirs with an average effective porosities between 0.24 and 0.27, net to gross (NTG) averaging between 0.8 and 0.86. KUKO A has the highest stock tank oil initially in place (STOIIP) in the KUKO field. The Prospect T was also discovered by superimposing the attribute and the different static models generated. This study has therefore demonstrated that integrating 3D seismic, well log data and seismic attributes with a 3D static reservoir model is a feasible tool for accurately characterizing hydrocarbon reservoirs. However, additional data is required to facilitate comprehensive research endeavors such as sequence stratigraphic analysis and rock physics, which can significantly improve evaluation accuracy and minimize uncertainties, particularly concerning the petrophysical properties of the reservoir.

References

- Alao, P. A., Olabode S. O., Opeloye S. A. (2013). Integration of Seismic and Petrophysics to Characterize Reservoirs in “ALA” Oil Field, Niger Delta. *The Scientific World Journal*, Article ID 421720, Vol. 2013.
- Doust, H. (1989). The Niger Delta: hydrocarbon potential of a major Tertiary delta province. *Coastal Lowlands*, 203–212.
- Doust, H. and Omatsola, E. (1990). Niger Delta, in, Edwards J.D., and Santogrossi, P.A., eds., *Divergent/Passive Margin Basins*, A.A.P.G. memoir, 48: Tulsa, Association of Petroleum Geologists, p 239-248.
- Halderson, H. H. and Damsleth, E. (1993). Challenges in reservoir characterization. *Amer. Assoc. Pet. Geol. Bull.*, 77, 541–551.
- Magoon, L. B. and Dow, W. G. (1994). *The Petroleum System: From Source to Trap*. Amer Assn of Petroleum Geologists, p 76.
- Osaki, L. J., Etim D. U. and Alex O. (2018). Geomechanical reservoir model for Appraisal and Development of Emi-003 field In Niger Delta, Nigeria *Asian Journal of Applied Science and Technology: Volume 2, Issue 4*, p. 276-294.
- Rahmadi, H. (2010). *Petrel course: Basic seismic interpretation introduction*, Geomodelling research group, pp. 35.
- Yuan, Z. M., Xinghe, Y., Paul, L. P., Ernest, G. and Shengli L. (2011). Reservoir characterization and modeling: A look back to see the way forward, in Y. Z. Ma and P. R. La Pointe, eds., *Uncertainty analysis and reservoir modeling: AAPG Memoir 96*, p. 289 – 309.

